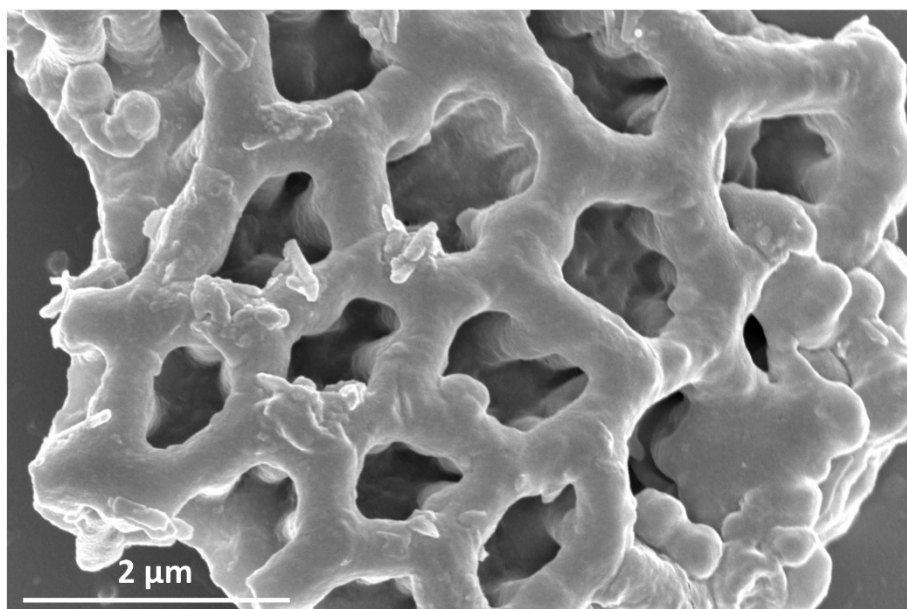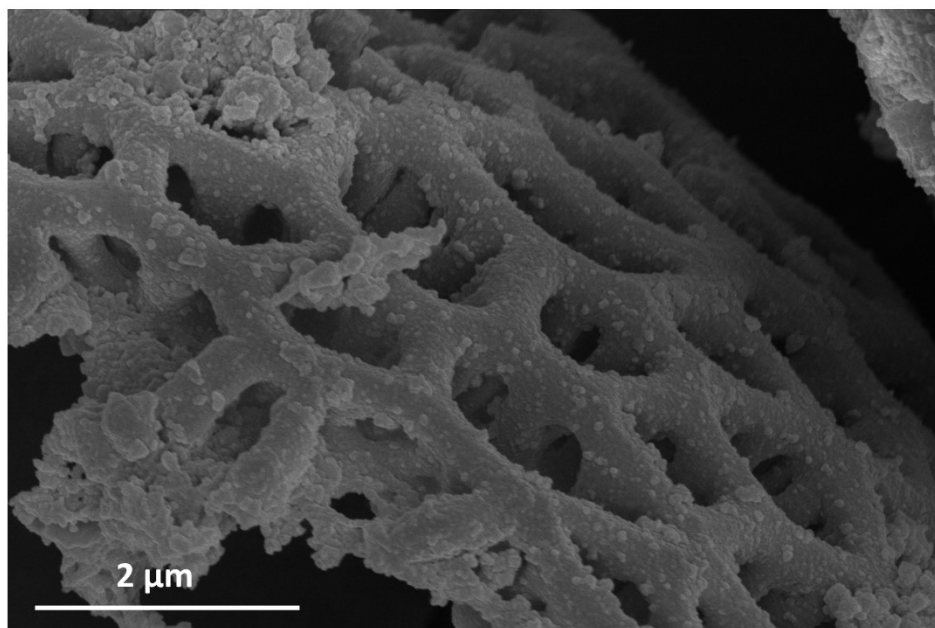**Supporting Information**

Figure S1. Sem of rape pollen.
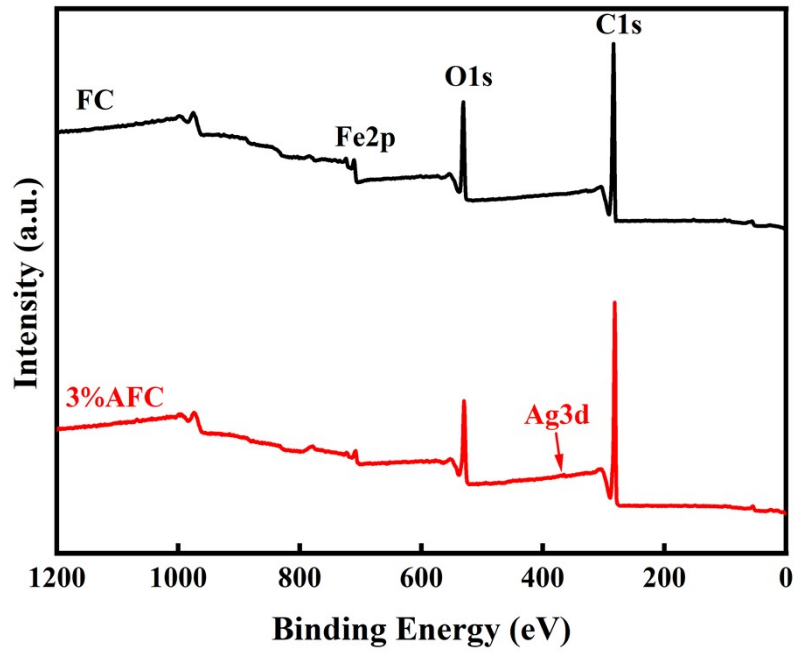
Figure S2. Sem of treated pollen.

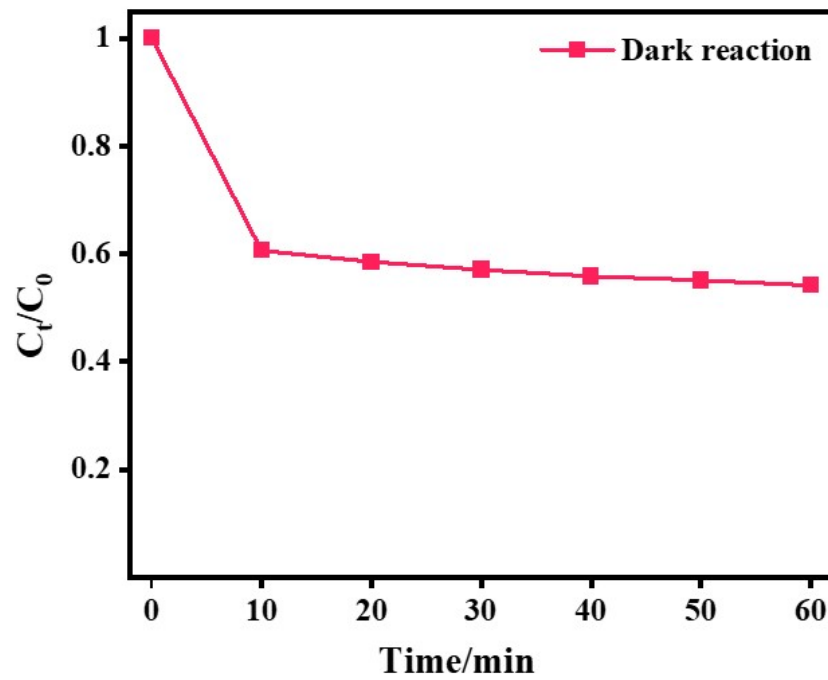**Figure S3.** Full XPS spectra of FC with 3% AFC photocatalysts.

Figure S4. 3%AFC adsorption kinetic curves for the dark reaction.

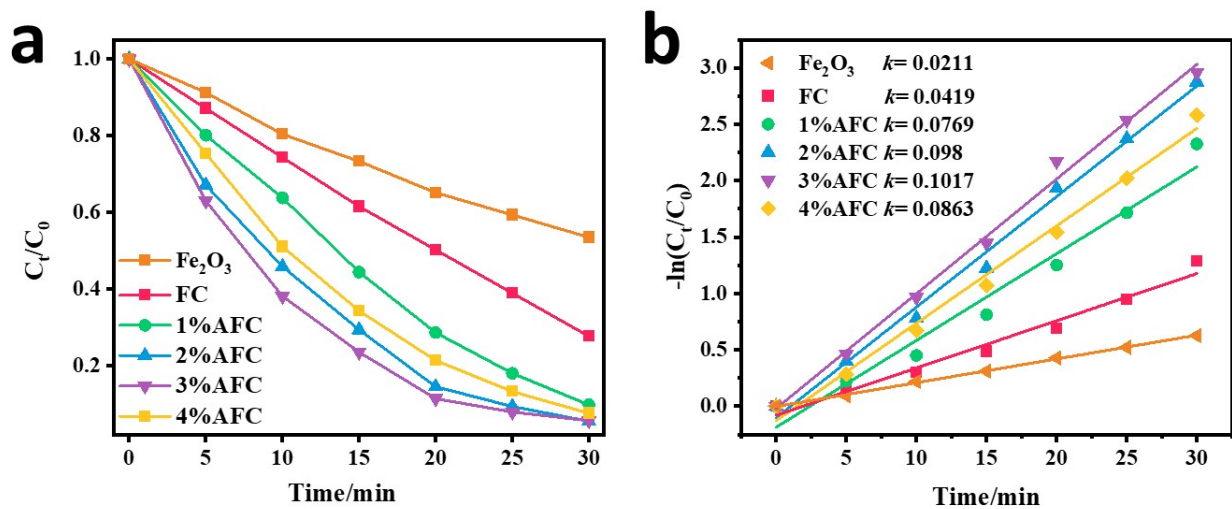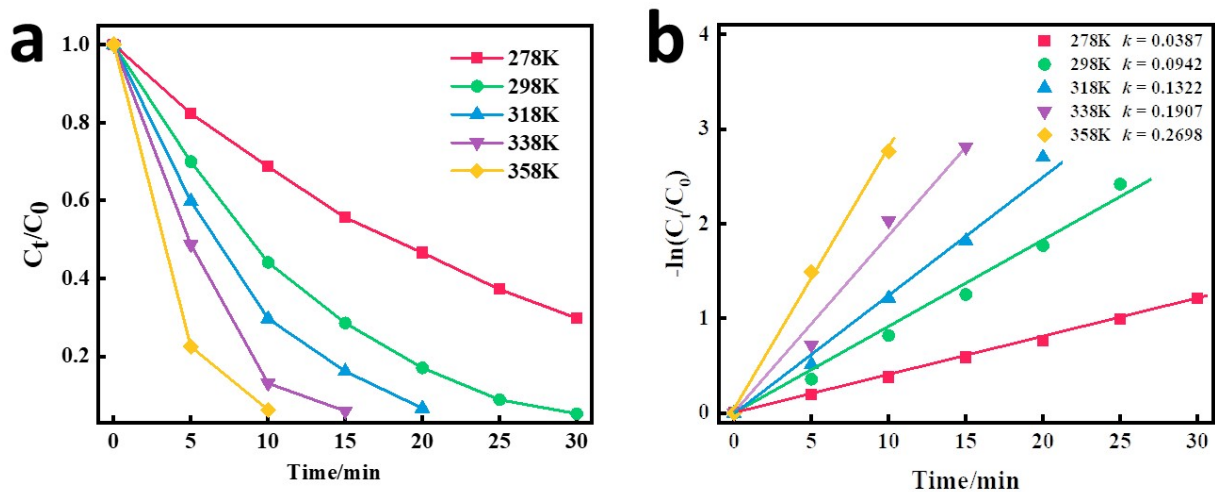**Figure S5.** MB photodegradation kinetic curves (a), and pseudo-primary kinetic

curves (b) with different photocatalysts.

Figure S6. 3%AFC degradation of MB under different reaction temperature (a) and
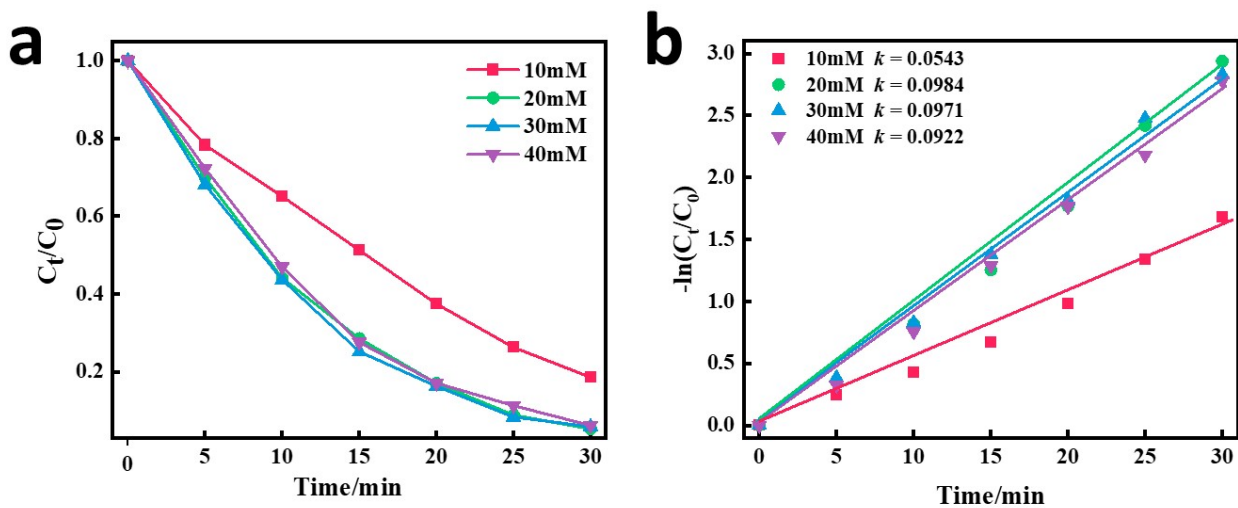
pseudo primary kinetic curve (b).

Figure S7. 3%AFC degradation of MB under different H_2O_2 concentration (a) and
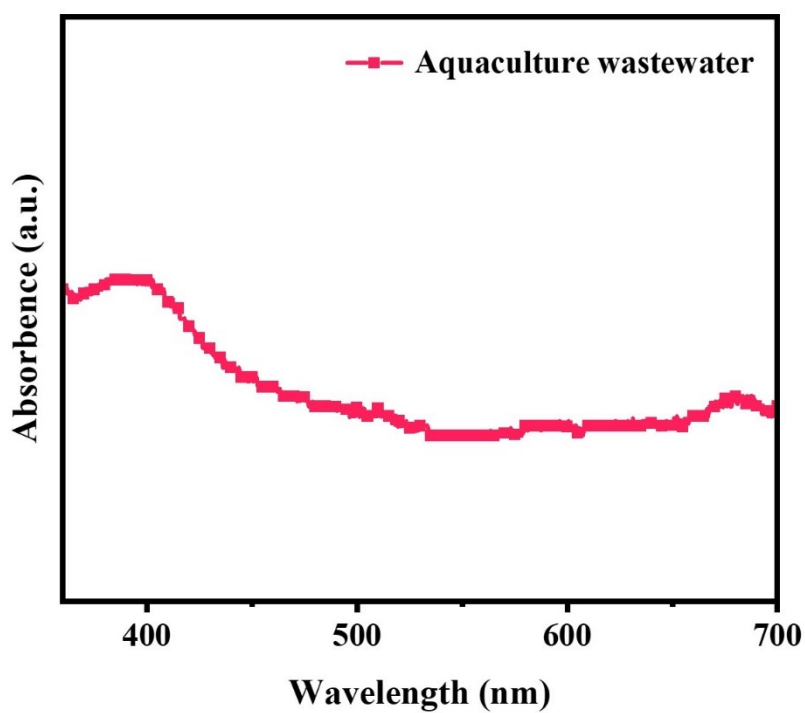
pseudo primary kinetic curve (b).

Figure S8. Absorbance curves of aquaculture wastewater.

Text S1. Chemicals and characterizations

All chemicals used were of analytical grade and required no further purification. Formaldehyde, sodium hydroxide, sodium fluoride, H_2O_2 (30 wt%), $Fe(NO_3)_3 \cdot 9H_2O$, anhydrous ethanol, sodium ethylenediaminetetraacetate (EDTA-2Na), methyl orange, and neutral red were procured from Guangzhou Guanghua Science and Technology Co., Ltd. Sulfuric acid and hydrochloric acid were obtained from Chengdu Xilong Scientific Co., Ltd. Cetyltrimethylammonium bromide (CTAB), polyethylene glycol, and isopropanol were sourced from Shanghai Aladdin Biochemical Technology Co., Ltd. Methylene blue (MB), Rhodamine B (RhB), acid orange, and p-benzoquinone were purchased from Shanghai Macklin Biochemical Co., Ltd. Silver nitrate ($AgNO_3$) was acquired from Tianjin Kemiou Chemical Reagent Co., Ltd.

Text S2. Catalytic performance evaluation.

In the photo-Fenton degradation assay, methylene blue (MB) at a concentration of 2 mg was introduced into 200 mL of ultrapure water, with the mixture subsequently agitated for 30 minutes. The solution's pH was meticulously adjusted to 7.0 utilizing hydrochloric acid (HCL) and sodium hydroxide (NaOH) then transferred to a 200 mL photoreactive chamber. A 20mg quantity of the catalyst was added, followed by a 30-minute dark, stirring period to establish a dynamic equilibrium between adsorption and desorption processes. After that, 20.0 mM hydrogen peroxide (30.0 wt%) was incorporated to initiate the photo-Fenton reaction under visible light conditions. Illumination was provided by a 300W xenon lamp (PLS-SXE300, Beijing Perfectlight)

equipped with a wavelength cutoff filter ($\lambda > 420$ nm), delivering an intensity of 122.5 mW/cm² at a 25 cm distance from the reactor. Temperature regulation was achieved using an external low-temperature thermostat to mitigate thermal effects from the light source. Control experiments were performed by altering a single reaction parameter to elucidate the influence of various conditions on the photo-Fenton process. Samples of 4 mL were extracted every 5 minutes and centrifuged, and the clarified supernatant was subsequently analyzed via UV-visible spectrophotometry to ascertain the residual concentration of MB. In the scavenging tests for reactive oxygen species (ROS), 1 mM solutions of EDTA-2Na, $AgNO_3$, isopropanol, and 1,4-benzoquinone served as quenchers for h^+, e^-, $\cdot OH$, and $\cdot O_2^-$ radicals, respectively. Degradation efficiency and the primary kinetic curve of photocatalytic degradation is calculated by the following equation was quantified using the following percentage calculation:

$$\text{Degradation efficiency} = \frac{C_t}{C_0} \times 100\% \tag{1}$$

$$-\ln(C_t/C_0) = \kappa t \tag{2}$$

The C_0 is the initial absorbance of the sample, and C_t is the absorbance at time t.

Text S3. Photo-Fenton Bacteriostatic Process

Escherichia coli was cultured in LB medium for 18 hours to reach the stationary phase. The bacterial concentration (OD600) was then diluted to 0.05, resulting in an initial viable cell density of 10^6 CFU/mL. The bacterial suspension was transferred to sterilized photocatalytic containers, and a photocatalyst was added at a concentration of 100 mg/L. The pH of the solution was adjusted using a pH adjuster. The mixture was

stirred in the dark for 20 minutes to achieve dynamic adsorption equilibrium. Then, 20 mM H2O2 solution was added. Under light irradiation, 1 mL of the bacterial suspension was collected at time points of 0, 3, 6, 9, 15, and 30 minutes, appropriately diluted, and spread on LB agar plates. The plates were incubated at 37°C for 24 hours, and the number of colonies was counted. The bactericidal ability of the composite material under photo-Fenton conditions was determined based on the change in the number of colonies.

Text S4. Analytical methods.

The catalytic activity of the composite materials was measured using a UV-visible spectrophotometer (UV Hitachi U-3900H). The morphology of the prepared samples was characterized by field emission scanning electron microscopy (FESEM, JEOL JSM-7800) and transmission electron microscopy (TEM, JEOL JEM 2100). Elemental percentage analysis was conducted with an energy-dispersive X-ray detector (EDS). The crystal structure of the composite materials was determined by analyzing X-ray diffraction (XRD) patterns with an X-ray diffractometer (D8 ADVANCE A25). X-ray photoelectron spectroscopy (XPS, AXISULTRA) detected the samples' chemical composition. The molecular structure of the materials was investigated using Fourier-transform infrared spectroscopy (FT-IR vertex70). The optical absorption properties of the composite materials were obtained by UV-visible diffuse reflectance spectroscopy (UV Hitachi U-3900H). The optical properties of the composite materials were acquired using a photoluminescence spectrophotometer (PL, Shimadzu RF-6000). All electrochemical experiments were performed at a Corrtest (CS350) electrochemical

workstation. Electron paramagnetic resonance (EPR) spectra were obtained using an EMX-8 instrument from Bruker, Germany.

SEM analysis: In this experiment, the sample was added to anhydrous ethanol and ultrasonically dispersed for 3 minutes. Using a disposable dropper, the dispersed ethanol-catalyst mixed solution was dropped onto the surface of a silicon wafer. After the ethanol completely evaporated, the silicon wafer containing the sample was placed on the SEM sample stage for observation and analysis.

TEM analysis: In this experiment, the sample material was added to anhydrous ethanol and ultrasonically dispersed for 3 minutes. Using a disposable dropper, the dispersed ethanol-catalyst mixed solution was dropped onto the surface of a microgrid. After the ethanol completely evaporated, the microgrid loaded with the catalyst was placed on the TEM sample platform for observation and analysis.

UV-Vis Diffuse Reflectance: In this experiment, barium sulfate was selected as the reference substrate for testing. The UV-Vis diffuse reflectance spectra of the sample material were collected using a Hitachi U-3900H spectrophotometer within the wavelength range of 300~800 nm.

XRD analysis: This experiment used an X-ray diffractometer with a Cu target as the radiation source. The operating voltage was 40 KV, the current was 40 mA, the diffraction angle ranged from 10-90°, and the scanning rate was 10°/min.

FT-IR analysis: The experiment used the potassium bromide (KBr) pellet method to process the material sample. The photocatalyst and KBr were ground and mixed evenly,

then pressed into transparent pellets under a pellet press. Infrared spectral analysis was conducted within the 400-4000 cm^{-1} range.

BET analysis: The experiment determined the specific surface area of the sample by measuring the N^2 adsorption/desorption isotherms at 77 K. After degassing at 105°C for 6 hours using an accelerated surface area and porosimeter analyzer.

Electrochemical Workstation: The experiment prepared the sample working electrode by dispersing 4 mg of photocatalyst and 40 μL of Nafion solution (5 wt%) in 1 mL of a solution with a 3:1 volume ratio of isopropanol to water. Ultrasonic treatment for at least 60 minutes formed a uniform ink. The mixed solution was then evenly dropped onto a conductive glass electrode (FTO), creating a photocatalyst loading of 0.6 mg/cm² on the FTO glass. The experiment used a platinum sheet as the reference electrode and NaSO3 as the electrolyte in the reaction cell, with a working voltage range of -2 to 1 V.

PL: The experiment selected 550 nm as the excitation wavelength and recorded the photoluminescence spectrum of the photocatalyst between 775-875 nm.

EPR analysis: The experiment used 5,5-dimethyl-1-pyrroline N-oxide (DMPO) as the spin trapping agent to capture ·OH and ·O2- radicals generated in the reaction system, forming spin adducts. An electron spin resonance spectrometer detected these adducts. The EPR operating parameters included a center field strength of 351.184 mT and a microwave frequency of 9.77 GHz.

Catalyst	Organic species	Catalyst dosage	H_2O_2 dosage	T (min)	Degradation rate (%)	Lamp source	Reference
$Fe_2O_3/ZnFe_2O_4/Mn_2O_3$	MB	50mg	-	30	99%	300W Xe lamp	[1]
Fe_2O_3 QDs/g-C_3N_4	TC	20 mg	3mL	60min	90%	300W Xe lamp	[2]
Fe_2O_3 QDs/3D g-C_3N_4	Phenol	40mg	900μL	240min	99%	500W Halogen lamp	[3]
Fe_2O_3/Sn	RhB	10mg	255μL	150min	100%	300W Xe lamp	[4]
Fe_2O_3/TiO_2/BC	MB	20mg	2mL	60min	99%	-	[5]
Ag@Fe_2O_3/C	MB	20mg	400μL	30min	99%	300W Xe lamp	This Work

Table S1. Comparison of the performance of Ag@Fe_2O_3/C in this study with that of other recently reported high-performance photocatalysts for the Photo-Fenton degradation of wastewater.

REFERENCES

[1] Lei, Y.; Wang, J.; Jiang, B.; Liu, H.; Lan, H.; Zhang, Y.; Gao, G. Enhanced photo-Fenton degradation of contaminants in a wide pH range via synergistic interaction between 1T and 2H MoS_2 and copolymer tea polyphenols/polypyrrole. J Colloid Interface Sci 2024, 658, 74-89.

[2] Wang, L.; Liu, S.; Lu, J.; Yuan, Z.; Gao, D.; Li, Y. Construction of $ZnFe_2O_4$/g-C_3N_4 nanocomposite catalyst for degradation of organic compound through photodegradation and heterogeneous Fenton oxidation. Materials Today Sustainability 2023, 24.

[3] Liu, D.; Li, C.; Ni, T.; Gao, R.; Ge, J.; Zhang, F.; Wu, W.; Li, J.; Zhao, Q. 3D interconnected porous g-C_3N_4 hybridized with Fe_2O_3 quantum dots for enhanced photo-Fenton performance. Applied Surface Science 2021, 555.

[4] Popov, N.; Ristić, M.; Bošković, M.; Perović, M.; Musić, S.; Stanković, D.; Krehula, S. Influence of Sn doping on the structural, magnetic, optical and photocatalytic properties of hematite (α-Fe_2O_3) nanoparticles. Journal of Physics and Chemistry of Solids 2022, 161.

[5] Chen, X. L.; Li, F.; Chen, H.; Wang, H.; Li, G. Fe_2O_3/TiO_2 functionalized biochar as a heterogeneous catalyst for dyes degradation in water under Fenton processes. Journal of Environmental Chemical Engineering 2020, 8 (4).